IEEE Access
Multidisciplinary | Rapid Review | Open Access Journal

Received November 25, 2020, accepted January 19, 2021, date of publication January 29, 2021, date of current version February 26, 2021.

Digital Object Identifier 10.1109/ACCESS.2021.3055637

DSC-ESO Approach to Robust Sliding Model Control for Ship's Curve Trajectory Tracking

JUN NING[1], HANMIN CHEN[1], WEI LI[1], AND BAISONG DU[2]
[1]Navigation College, Dalian Maritime University, Dalian 116026, China
[2]School of Port and Transportation Engineering, Zhejiang Ocean University, Zhoushan 316022, China

Corresponding author: Jun Ning (junning@dlmu.edu.cn)

This work was supported in part by the National Natural Science Foundation of China under Grant 51939001, Grant 61976033, Grant U1813203, Grant 61803064, and Grant 61751202; in part by the Science and Technology Innovation Funds of Dalian under Grant 2018J11CY022; and in part by the Natural Science Foundation of Liaoning Province under Grant 20170540098.

ABSTRACT In order to solve the problem of ship's curve trajectory-tracking control, the Norrbin nonlinear response model which can accurately describe the ship's motion state is selected in this paper. The hyperbolic tangent function is used to design the expected hemispheric angle equation, then the complex track control is transformed into a heading control problem. The fast terminal sliding mode (FTSM) is introduced together with the Backstepping control technique to reduce the system adjustment time, eliminate the chattering. Bying combined with extended states observer (ESO) and dynamic surface control (DSC) technique, the internal and external disturbances in real-time can be estimated and compensated, and the ''explosion of complexity'' caused by backstepping technique is solved. The state of the control system is bounded and stable, and the system error converges to zero. Matlab simulation proves that the controller can realize the trajectory-tracking control quickly and accurately, and has strong robustness to external disturbances.

INDEX TERMS Fast terminal sliding mode, extended states observer, ship trajectory-tracking control, robustness.

I. INTRODUCTION

With the rapid development of automation technology [1]–[8], ship automation [9], [10] has begun to receive attention widely. As one of the vital research objects of ship automation technology, efficient ship motion control [11], [12] can significantly improve the safety of the ship and increase the economic benefits during the navigation. In light of this, it is necessary to accelerate research on ship motion control. As is known to all, the study of ship motion control includes ship's characteristics(such as non-linearity, large inertia, maneuvering delay, multiple degree-of-freedom) [13], [14], and the aspects of motion control(such as external environmental interference, input saturation, parametric uncertainty, model accuracy) [15], [16]. In evidence, the reasons mentioned above bring significant challenges to the research [17].

In recent years, many researchers have studied the problem of the ship heading control extensively. Due to improving the control performance of the ship course, Chen *et al.* [18] proposed an adaptive linear active disturbance rejection control (LADRC) controller based on Q-learning algorithm, and it can effectively avoid the parameter tuning process. Based on the identified ship plant and the cloud model, Zhu *et al.* [19] put forward new approaches on system identification and controller design to study ship course-keeping, and the support vector machines(SVM) which optimized by artificial bee colony algorithm(ABC) was applied to estimate the parameters of the control model. Liu [20] also addressed the problem of course keeping, and chose the feedback linearization method to simplify the nonlinear system. Besides, the disturbance observer technique is applied to ensure the robust performance of the time-varying wave moment and actuator dynamics. An adaptive self-regulation proportion integration differentiation (PID) scheme is also proposed to resolve the problem of ship course control in [21], and without depending on model parameters and unknown input.

However, the above researches are not involved in the ship trajectory tracking. And trajectory-tracking has always been a difficulty in the study of ship motion control. Given that, Ma *et al.* [22] proposed an adaptive neural network (NN) trajectory tracking control scheme, wherein a nonlinear error-driven function was employed to eliminate the input saturation's effect and improve the stability

The associate editor coordinating the review of this manuscript and approving it for publication was Haiyong Zheng.

of the control system. To resolve the ship trajectory tracking problem, Wang *et al.* [23] proposed a finite-time fault estimator based fault-tolerance control (FFE-FTC) scheme, which consists of the integral sliding mode control method and Nussbaum technique. By using the sliding mode control theory, Sun *et al.* [24] proposed a virtual control point method to resolve the ship trajectory tracking problem and ensure position tracking with a desired velocity. For the problem of track deviation influenced by diverse interference, Chen *et al.* [25] put forward an adaptive NN trajectory tracking control scheme, and then it can effectively address the input saturation that exists in the realistic situation. Due to dealing with the non-linearity of the ship, Li *et al.* [26] proposed an adaptive NN finite-time fast reaching law based on the backstepping method, which can also increase the convergence rate of tracking error while the convergence error can reach to zero in a finite time.

On the other side, it is easy to cause the repeated derivative of virtual law when using the backstepping technology, and then makes the design process of motion control more complicated in practice. By using the neural network and dynamic surface control method, a robust control scheme was designed in [27], wherein the problem of complicated explosion with traditional backstepping was avoided. Combined with a smooth hyperbolic tangent function, Shen *et al.* [28] present a minimum learning parameter(MLP) neural network-based recursive sliding mode dynamic surface control scheme, and the Nussbaum function was employed to compensate for the saturation function and ensure the stability of the system. Based on the dynamic surface control method, Li [29] introduced two novel coordinate transformations to deal with the problems caused by the non-zero off-diagonal terms in the inertia matrix and the underactuation. By introducing a first-order low-pass filter in each step of the backstepping method, the dynamic surface control method overcomes the "explosion of complexity" in the traditional backstepping process.

It is general that the external ocean interferences such as wind and wave, which can obviously make the ship off track, are unavoidable during the navigation. However, in [27], [29], external interferences are not considered globally. Following that, a DSC-ESO approach based on the sliding mode control is proposed for the surface ship with external environmental interference, input saturation, and parametric uncertainty in this paper. The Norrbin nonlinear response model, which can accurately describe the ship's motion state, is selected. The hyperbolic tangent function is used to design the expected hemispheric angle equation and effectively limit the control input. The extended state observer is utilized to evaluate the external disturbance and simplify the design process of trajectory tracking. The fast terminal sliding mode (FTSM) is used to address the problem of traditional sliding mode control and stabilize the tracking errors in finite-time. Matlab simulation proves that the controller can realize the trajectory-tracking control quickly and accurately, and has strong robustness to external disturbances. Main contributions of this paper are summarized as follows:

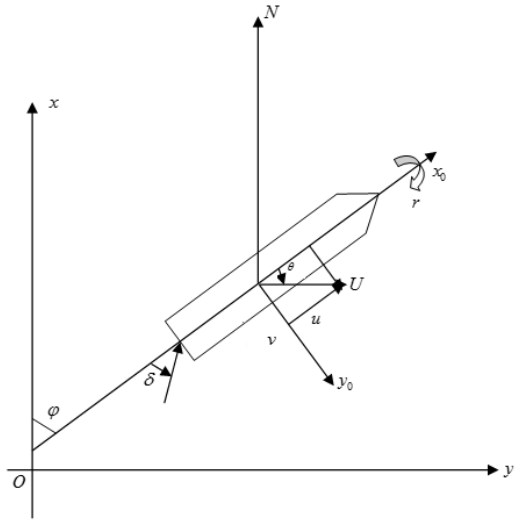

FIGURE 1. Ship plane motion schematic and variable.

(1) The hyperbolic tangent function transforms the sophisticated track control into the heading control problem and addresses the issue of input saturation.

(2) By combined with extended state observer (ESO) and dynamic surface control (DSC) technique, the internal and external disturbances in real-time can be estimated and compensated, and the "explosion of complexity" caused by backstepping technology is solved. The state of the control system is bounded and stable, and the system error converges to zero.

(3) The fast terminal sliding mode (FTSM) is introduced in Backstepping control to reduce the system adjustment time, eliminate the chattering.

The remainder of this paper is organized as follows. The mathematical model of ship motion control is introduced in Section II. and the ship track control method is also presented in this part. The controller design and stability analysis are addressed in Section III. The effectiveness of the proposed method is validated by simulation in Section IV. This brief ends with conclusions drawn in Section V.

II. PRELIMINARIES

A. MATHEMATICAL MODEL OF SHIP MOTION

For the majority of ship motion control problems, such as course control, track control, dynamic positioning and automatic collision avoidance, the pitching rate, rolling rate and heave velocity can be ignored. Only the surge velocity, sway velocity and yaw rate are considered, thus reducing the ship's 6 DOF (degree of freedom) to 3 DOF plane motion control [22]. As shown in Figure 1:

Usually, the ship is driven by the rudder and propeller to achieve forward, lateral drift and bowing. This kind of ship which driving force is less than the degree of freedom, that is, the underactuated ship. Underactuated ships are vulnerable to external interference and it is difficult to control course angle and eliminate track deviation simultaneously.

First, consider the simplest form of ship motion Nomoto model [30]

$$\ddot{\psi} + \frac{1}{T}\dot{\psi} = \frac{K}{T}\delta \tag{1}$$

Considering the ship's nonlinearity, $\frac{1}{T}\dot{\psi}$ should be represented by a nonlinear term $\frac{K}{T}H(\dot{\psi})$.

$$H(\dot{\psi}) = \alpha'\dot{\psi}^3 + \beta\dot{\psi} \tag{2}$$

α', β are the proportional coefficient of yaw rate, K and T are the ship maneuverability indexes, and the values of α', β, K, T are all related to ship's speed. $\dot{\psi}$ denotes the derivative of heading angle.

Then formula (1) can be expressed as:

$$\ddot{\psi} + \frac{K}{T}H(\dot{\psi}) = \frac{K}{T}\delta \tag{3}$$

Combining the kinematic and dynamic characteristics of the ship, also considering the influence of external wind, wave and current, formula (3) can be expressed into a second-order Norbrin nonlinear response model, which can accurately describe the ship's motion state [31]:

$$\begin{cases} \dot{\psi} = r \\ \dot{r} = f(r) + b\delta + w(t) \end{cases} \tag{4}$$

$f(r) = -a_1 r - a_2 r^3, a_1 = -K^*\beta/T, a_2 = \alpha' K/T, b = K/T, w(t)$ is the external interference, r is the ship's yaw rate, δ is the rudder angle.

The relationship between the position and the motion parameters of the ship can be expressed by the following equations [32]:

$$\begin{cases} \dot{x} = u\cos\psi - v\sin\psi \\ \dot{y} = u\sin\psi + v\cos\psi \end{cases} \tag{5}$$

x and y are the longitudinal and lateral positions of the ship in the inertial coordinate system, u is the surge velocity, v is the sway velocity.

In order to achieve the command rudder angle quickly and accurately reach the desired angle, it is necessary to consider the characteristics of the ship servo system. The servo characteristics are generally expressed by the following first-order inertia system [31]:

$$\dot{\delta} = K_E\left(\delta_E - \delta\right)/T_E \tag{6}$$

K_E is the servo control gain, T_E is the time constant, and δ_E is the command rudder angle.

B. SHIP TRAJECTORY-TRACKING CONTROL METHOD

Considering the nonlinear mathematical model of ship track control system with external interference composed of equations (4), (5) and (6), it is as follows:

$$\begin{cases} \dot{x} = u\cos\psi - v\sin\psi \\ \dot{y} = u\sin\psi + v\cos\psi \\ \dot{\psi} = r \\ \dot{r} = -a_1 r - a_2 r^3 + b\delta + w \\ \dot{\delta} = K_E\left(\delta_E - \delta\right)/T_E \end{cases} \tag{7}$$

In this paper, the indirect trajectory control method is addressed by using the method proposed in [33]. By constructing the expected heading equation $\psi_d(t)$, the heading is consistent with the desired heading, then $\psi \to \psi_d$, and the trajectory deviation is reduced to zero. Because the longitudinal deviation can be eliminated by advancing or reversing, this paper only to consider eliminating the lateral position deviation.

The expected heading equations are as follows [32]:

$$\begin{cases} \Delta\dot{y} = u\sin\Delta\psi + v\cos\Delta\psi \\ \Delta\psi = \psi - \psi_p \\ \Delta\psi_d = -l_2\int_0^t \tanh[\Delta\dot{y}(\delta) + l_1\tanh(l_0\Delta y)]d\delta \\ \psi_d(t) = \Delta\psi_d + \psi_p \end{cases} \tag{8}$$

In the equation (8), Δy is the lateral position deviation, ψ is the actual heading angle, ψ_p is desired heading, l_0, l_1, l_2 are the parameters to be determined and $l_0, l_1, l_2 > 0$. Where, l_0 can compress the lateral deviation of the ship in the course of traveling, l_1 can adjust the convergence speed of the track error, and l_2 can adjust the speed of the integration process.

Equation (7) can make $\psi \to \psi_d$ and the track deviation converges to zero, proof as follows:

Because of $\Delta\dot{y} = u\sin\Delta\psi + v\cos\Delta\psi$, exists $\Delta\psi^* \in (-\frac{\pi}{2}, \frac{\pi}{2})$, makes function $g = u\sin\Delta\psi + v\cos\Delta\psi + l_1\tanh(l_0\Delta y) = \Delta\dot{y} + l_1\tanh(l_0\Delta y) = 0$ become ture,

$$\Delta\dot{y} = -l_1\tanh(l_0\Delta y) \tag{9}$$

Define the Lyapunov function $V = \frac{1}{2}\Delta y^2$

$$\dot{V} = \Delta y\Delta\dot{y} = -\Delta y l_1\tanh(l_0\Delta y) < 0 \tag{10}$$

So when $g = 0$, $\lim_{t\to\infty}\Delta y = 0$.

Then the lateral position deviation can converge to zero under the action of $\Delta\psi^*$.

When the $\Delta\psi \in (-\frac{\pi}{2}, \frac{\pi}{2})$, $\frac{\partial g}{\partial(\Delta\psi)} > 0$, that is, $g(\Delta\psi)$ is a monotonically increasing function.

Assume that $\psi_p = 0$, then $\Delta\psi = \psi, \Delta\psi^* = \psi^*, \Delta r = r$.

So when $\psi > \psi^*$, $g(\Delta\psi) > g(\Delta\psi^*) = 0$, and $\dot{\psi} = r = -l_2\tanh(g(\Delta\psi)) < 0$.

When $\psi < \psi^*$, $\Delta\psi < \Delta\psi^*$, $g(\Delta\psi) < g(\Delta\psi^*) = 0$, and $\dot{\psi} = r = -l_2\tanh(g(\Delta\psi)) > 0$.

The above process indicates that ψ^* can make the ship position deviation approach to zero, when $\psi > \psi^*, r < 0$, $\psi \to \psi^*, g = 0$, $\lim_{t\to\infty}\Delta y = 0$, when $\psi < \psi^*, r > 0$, $\psi \to \psi^*, g = 0$, $\lim_{t\to\infty}\Delta y = 0$.

Therefore, regardless of the state of the ship, the ship can track to the desired heading angle under the action of equation (7), and eliminate the track deviation.

III. CONTROLLER DESIGN AND STABILITY ANALYSIS

Based on the ship trajectory-tracking control method and mathematical model of ship motion mentioned above, this part carries out the controller design of the underactuated ship and stability analysis. The expected heading angle equation is designed by using the hyperbolic tangent function, and the equation is taken as the input of the controller, so that the

ship can constantly correct the heading error and ensure the real-time tracking of the expected heading angle and steer along the planned track. Based on the sliding mode control algorithm, the fast terminal sliding mode (FTSM) is adopted for better able to eliminate the phenomenon of sliding mode chattering, and reduce the system adjusting time. Moreover a continuous terminal attracting control law is designed, and the extended states observer (ESO) is used to observe the real-time system total disturbance, and then compensate into the control law. The stability analysis verifies the effectiveness of the proposed ESO-BFTSM tracking autopilot, and the system error convergence to an infinitesimal.

Without loss of generality, the following assumption and lemma are brought in for the use of the following parts [34].

Assumption 1: Assume the system reference signal $y_d(t)$ is a sufficiently smooth function of t, moreover, y_d and the derivatives $\dot{y}_d$, $\ddot{y}_d$ are also bounded, namely, a positive constant B_0 exists:

$$\Pi_0 := \left\{ \left(y_d, \dot{y}_d, \ddot{y}_d\right) : (y_d)^2 + (\dot{y}_d)^2 + (\ddot{y}_d)^2 < B_0 \right\} \quad (11)$$

Lemma 1: If the Lyapunov function $V(t,x)$ is positive definite, and $\dot{V}(t,x) \leq -k_1 V(t,x) + k_2$, where $k_1 \geq 0, k_2 \geq 0$ are the bounded constant, then

$$V(t,x) \leq \frac{k_2}{k_1} + \left[V(0) - \frac{k_2}{k_1} \right] e^{-k_1 t} \quad (12)$$

Lemma 2 (Barbalat's Lemma): If function $f(t)$ is uniformly continuous and $\lim_{t\to\infty} \int_0^t f(\tau) d\tau$ exists and bounded, then $\lim_{t\to\infty} f(t) \to 0$.

A. LINEAR EXTENDED STATES OBSERVER DESIGN

ESO is an essential part of Active Disturbances Rejection control(ADRC). It can estimate and compensate various disturbances in real-time without relying on specific mathematical models.

Considering the second-order nonlinear system (1), $f(r) + w(t) = h$. h which express the expansion state, is the sum of the uncertain interference, assume there is a derivative of h, define $\dot{h} = c$, and c is bounded, namely, a positive unknown constant J exists and $|c| < J$. Then the system (1) can be expanded into the form of the following state space:

$$\begin{cases} \dot{\psi} = r \\ \dot{r} = h + bu(t) \\ \dot{h} = c \\ y = \psi \end{cases} \quad (13)$$

According to the reference [33], the linear extended state observers (LESO) of equation (13) are as follows:

$$\begin{cases} \dot{z}_1 = z_2 - \dfrac{l_3}{w_0} e \\ \dot{z}_2 = z_3 - \dfrac{l_4}{w_0^2} e + bu(t) \\ \dot{z}_3 = -\dfrac{l_5}{w_0^3} e \\ e = z_1 - \psi \end{cases} \quad (14)$$

In the equation (14), $z = [z_1\ z_2\ z_3]^T$ are the estimates of ψ, r, h. $w_0 > 0$, l_3, l_4, l_5 are the positive constants, and $(s+1)^3 = s^3 + l_3 s^2 + l_4 s + l_5$ satisfy the Hurwitz condition.

Define the observation error $\xi = [\xi_1\ \xi_2\ \xi_3]^T$, and $\xi_1 = \frac{\tilde{z}_1}{w_0^2}$, $\xi_2 = \frac{\tilde{z}_2}{w_0}$, $\xi_3 = \tilde{z}_3$. $\tilde{z}_1 = \psi - z_1$, $\tilde{z}_2 = r - z_2$, $\tilde{z}_3 = h - z_3$.

Then,

$$\begin{aligned} w_0 \dot{\xi}_1 &= \frac{\dot{\tilde{z}}_1}{w_0} = \frac{r - \dot{z}_1}{w_0} = \frac{r - (z_2 - l_3(z_1 - y))}{w_0} \\ &= \frac{r - \left(z_2 + \frac{l_3}{w_0}\tilde{z}_1\right)}{w_0} = \frac{r - z_2}{w_0} - \frac{l_3 \tilde{z}_1}{w_0^2} \\ &= \xi_2 - l_3 \xi_1 \end{aligned} \quad (15)$$

$$\begin{aligned} w_0 \dot{\xi}_2 &= \dot{\tilde{z}}_2 = \dot{r} - \dot{z}_2 = h + bu - z_3 + \frac{l_4}{w_0}(z_1 - y) - bu \\ &= h - z_3 - \frac{l_4}{w_0^2}\tilde{z}_1 = \tilde{z}_3 - \frac{l_4}{w_0^2}\tilde{z}_1 = \xi_3 - l_4 \xi_1 \end{aligned} \quad (16)$$

$$\begin{aligned} w_0 \dot{\xi}_3 &= w_0 \dot{\tilde{z}}_3 = w_0 \left(\dot{h} - \dot{z}_3\right) = w_0 \left(c + \frac{l_5}{w_0^3}(z_1 - y)\right) \\ &= w_0 \left(c - \frac{l_5}{w_0^3}\tilde{z}_1\right) = w_0 c - l_5 \xi_1 \end{aligned} \quad (17)$$

So, the equation of state of the observation error can be written as:

$$w_0 \dot{\xi} = \bar{A}\xi + w_0 \bar{B} c \quad (18)$$

In the equation (18), $\bar{A} = \begin{pmatrix} -l_3 & 1 & 0 \\ -l_4 & 0 & 1 \\ -l_5 & 0 & 0 \end{pmatrix}$, $\bar{B} = \begin{bmatrix} 0 \\ 0 \\ 1 \end{bmatrix}$.

$\bar{A}$ can satisfy the Hurwitz condition by chosing $l_i\ (i = 3, 4, 5)$. Then, for any given symmetric positive definite matrix Q, the existence of symmetric positive definite matrix P satisfies the following Lyapunov equation

$$\bar{A}^T P + P\bar{A} + Q = 0 \quad (19)$$

Define the Lyapunov function $V_0 = w_0 \xi^T P \xi$.

$$\begin{aligned} \dot{V}_0 &= w_0 \dot{\xi}^T P \xi + w_0 \xi^T P \dot{\xi} \\ &= \left(\bar{A}\xi + w_0 \bar{B} c\right)^T P \xi + \xi^T P \left(\bar{A}\xi + w_0 \bar{B} c\right) \\ &= \xi^T A^T P \xi + w_0 \left(\bar{B} c\right)^T P \xi + \xi^T P \bar{A} \xi + w_0 \xi^T P \bar{B} c \\ &= \xi^T \left(A^T P + P\bar{A}\right) \xi + 2 w_0 \xi^T P \bar{B} c \\ &\leq -\xi^T Q \xi + 2 w_0 \left\| P\bar{B} \right\| \cdot \|\xi\| \cdot |c| \end{aligned} \quad (20)$$

$$\dot{V}_0 \leq -\lambda_{\min}(Q) \|\xi\|^2 + 2 w_0 J \left\| P\bar{B} \right\| \|\xi\| \quad (21)$$

$\lambda_{\min}(Q)$ is the minimum eigenvalue of Q.

According to $\dot{V}_0 \leq 0$, the convergence condition of the observer can be written as follow:

$$\|\xi\| \leq \frac{2 w_0 J \left\| P\bar{B} \right\|}{\lambda_{\min}(Q)} \quad (22)$$

Therefore, the convergence rate of observation error ξ is related to parameter w_0. And w_0 is the only parameter that the observer needs to determine. Selecte the appropriate w_0 can accurately estimate ψ, r, h and realize real-time observation and compensation of the total disturbance of the system.

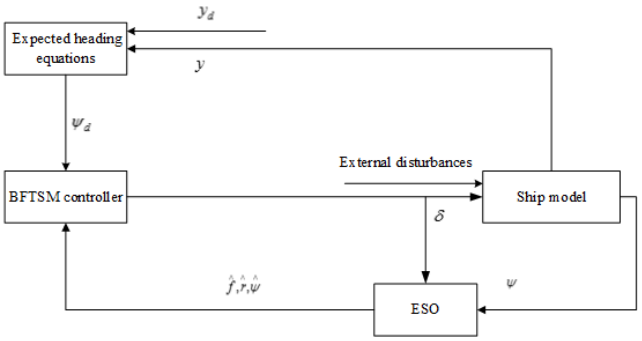

FIGURE 2. The block diagram of the designed control scheme

B. ESO-BFTSM CONTROLLER DESIGN AND STABILITY ANALYSIS

The purpose of the controller design is to combine the knowledge of Backstepping, FTSM and the ESO to design control law, so that the heading can track the expected heading equation, the track deviation converges to zero, and the control system is stable. And, the block diagram of the designed control scheme is given as follows.

First, define the systematic error equation as follows [29]:

$$\begin{cases} e_1 = \psi - \psi_d \\ e_2 = r - r_d \end{cases} \tag{23}$$

In the equation (23), ψ_d is the desired heading, r_d is the virtual control amount of the heading rate, which needs to be designed.

Step 1: Design the virtual control amount r_d:

$$r_d = -c_1 e_1 + \dot{\psi}_d \tag{24}$$

In the equation(24), $c_1 > 0$. In order to avoid the differential expansion of the r_d derivative in the backstepping design, the following low-pass filter is introduced to filter it [35]:

$$\tau \dot{r}_d + r_d = \bar{r}, \quad r_d(0) = \bar{r}(0) \tag{25}$$

In the equation (25), define $\bar{r} = -c_1 e_1 + \dot{\psi}_d$, τ is filter time constant, r_d is the filtered estimate of $\bar{r}$.

The filtered error and its derivative are:

$$R = r_d - \bar{r}, \quad \dot{R} = -\frac{R}{\tau} + \dot{\bar{r}} \tag{26}$$

Since the variables in the system (1) and their derivatives are bounded, there is a non-negative continuous function η makes $\left|\dot{\bar{r}}\right| = \left|\dot{R} + \frac{R}{\tau}\right| \leq \eta$, the following equation can be obtained by Young's inequality:

$$R\dot{R} \leq -\frac{R^2}{\tau} + |R|\,\eta \leq -\frac{R^2}{\tau} + R^2 + \frac{\eta^2}{4} \tag{27}$$

Define the Lyapunov function is:

$$V_1 = \frac{1}{2}e_1^2 + \frac{1}{2}R^2 \tag{28}$$

By taking the derivative the V_1:

$$\begin{aligned} \dot{V}_1 &= e_1\dot{e}_1 + R\dot{R} = e_1(-c_1 e_1 + e_2) + R\dot{R} \\ &\leq -c_1 e_1^2 + e_1 e_2 - \frac{R^2}{\tau} + R^2 + \frac{\eta^2}{4} \end{aligned} \tag{29}$$

If the design of the second step makes e_2 to converge to 0, then there are:

$$\dot{V}_1 \leq -kV_1 + c \tag{30}$$

In the equation (30): $k = 2\min\left\{-c_1, 1 - \frac{1}{\tau}\right\}$, $c = \frac{\eta^2}{4}$.

According to the equation (12) and (30),

$$0 \leq V_1(t) \leq V_1(0)e^{-kt} + \frac{c}{k} \leq V_1(0) + \frac{c}{k}, \quad \forall t \geq 0 \tag{31}$$

The above equations show:

(1) $(V_1 - \frac{c}{k})$ is the exponential decay, i.e., the $\lim_{t\to\infty} \int (V_1 - \frac{c}{k})dt$ presence and there is a limit.

(2) V_1 and $\dot{V}_1$ are bounded, V_1 is continuous, then $\lim_{t\to\infty} V_1 = \frac{c}{k}$ can be obtained by the Barbalat's lemma.

According to the above analyses, when e_2 converges to 0, the system state satisfies the semi-global bounded consistency condition, and the tracking error of the system meets: $e_1 \to 0, \psi \to \psi_d$ [29].

Step 2: In order to converge the state tracking error e_2 to 0, stabilize the system, accelerate the convergence speed and avoid the sliding mode chattering phenomenon. The following form of FTSM [36] is adopted:

$$s = \int_0^t e_2 d\tau + \alpha(\int_0^t e_2 d\tau)^{\gamma} + \beta e_2^{\lambda} \tag{32}$$

In the equation (32), $\gamma = k/h$, $\lambda = p/q$, k, h, p, q are positive odd numbers, $1 < \lambda < 2$, $\gamma > \lambda$, α and β are known as ordinary numbers. When the system state keeps approaching the sliding surface, the high-power term of the state tracking error integral $\int_0^t e_2 d\tau$ plays a fast attracting effect. The system state quickly reaches the sliding surface and slides on the surface, after that, the state tracking error integral term accelerates the steady speed, making the system error quickly converges to zero [32]. Since both γ and λ are positive numbers, the negative exponential term is not generated when the sliding surface is deduced, which eliminates the singular problem well [32].

According to the characteristics of the above FTSM, design the terminal attractor $\kappa = \beta\lambda e_2^{\lambda-1}$, and the continuous approach law is:

$$\dot{s} = -\kappa(\mu s^{m/n} + \eta s) \tag{33}$$

In the equation (33), m and n are positive numbers and $0 < m/n < 1$, $\mu > 0$, $\eta > 0$.

Then we have:

$$\begin{aligned} \dot{s} &= e_2 + \gamma\alpha(\int_0^t e_2 d\tau)^{\gamma-1} e_2 + \lambda\beta e_2^{\gamma-1}\dot{e}_2 \\ &= e_2 + \gamma\alpha(\int_0^t e_2 d\tau)^{\gamma-1} e_2 + \lambda\beta e_2^{\gamma-1}(f(r) + bu + w - \dot{\alpha}_1) \end{aligned} \tag{34}$$

By combining equations (33) and (34), the final BFTSM control law can be obtained:

$$\begin{aligned} u = -b^{-1}(z_3 - \dot{\alpha}_1 + (\lambda\beta)^{-1}(\gamma\alpha(\int_0^t e_2 d\tau)^{\gamma-1} e_2^{2-\gamma} + e_2^{2-\gamma}) \\ + e_2^{\lambda-\gamma}\left(\mu s^{m/n} + \eta s\right)) \end{aligned} \tag{35}$$

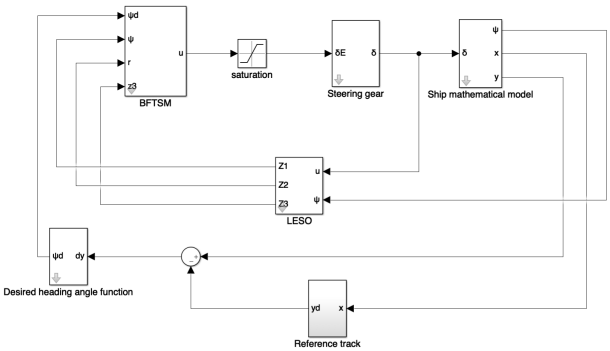

FIGURE 3. ESO-BFTSM controller structure.

In the equation (35), $z_3 \approx h = f(r) + w$ is the observation of the total disturbance of the system by the ESO in real-time.

Select the Lyapunov function $V_2 = \frac{1}{2}s^2$ and calculate its derivative:

$$\dot{V}_2 = s\dot{s} = s[-\kappa(\mu s^{m/n} + \eta s)] = -\beta\lambda e_2^{\lambda-1}(\mu s^{m/n+1} + \eta s^2) \tag{36}$$

When $s \neq 0$, $\lambda = p/q$, $0 < m/n < 1$, $1 < p/q < 2$, $\lambda = p/q$, since p, q, m, n are both positive odd numbers, $e_2^{\lambda-1} > 0$, $s^{m/n+1} > 0$, $\dot{V}_2 \leq 0$. Therefore, e_2 can be converged to 0 at a finite time.

Considere the whole closed-loop system, the Lyapunov function is:

$$V = V_0 + V_1 + V_2 \tag{37}$$

When e_2 converges to 0 and selecte the appropriate w_0,can ensure $\dot{V} \leq 0$, that is, all states of the system are semi-globally uniformly bounded [32], and the control system is progressively stable, achieving the purpose of trajectory tracking control.

IV. SIMULATION

In this part, a Matlab simulation experiment has been done based on the ocean-going training vessels YULONG which belongs to Dalian Maritime University. The Norrbin coefficitent and the indices of the Nomoto model will change with the ship's speed and loading status. Considering the model perturbation error and the limited simulation condition, in this thesis, the parameter values under economic speed are used as parameter inputs for simulation. The controller structure is shown in Figure 3. The length of "YULONG" is 126m, the ship's width is 20.8m, the full load draught is 8.0m, the square factor is 0.681, a = 30, the initial speed of the ship is v_0 = 7.2m/s, K = 0.478, T = 216 [31]. The parameters of the ship's expected heading equation are: $l_0 = 0.003, l_1 = 3, l_2 = 0.008$, the ESO parameter is $w_0 = 100$, the controller parameters are: $c_1 = 1, \tau = 3, \gamma = 7/5, \lambda = 9/7, \alpha = 1, \beta = 125, m/n = 53/55, \mu = 1, \eta = 0.01$.

Since the complex curve path can be decomposed into several sinusoids, the sinusoid with the amplitude of 300m and the frequency of $\pi/2500$ rad/sec is selected as the desired track, that is, $y_d = 300\sin(0.0004\pi x)$.

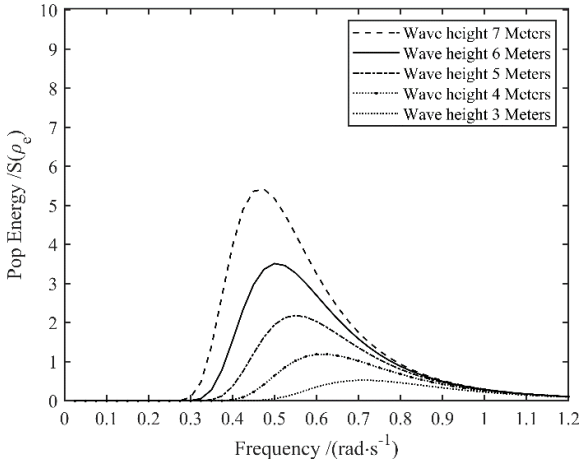

FIGURE 4. Spectrum corresponding different wave height.

The actual sea surface wave is highly irregular and has a lot of randomnesses, so the wave is usually treated as a random process. The casual wave spectrum can be used to describe the distribution of the internal energy of the wave in each wave unit and its interior distribution characteristics. The current typical wave spectrums include PM(Pierson–Moskowitz) spectrum, Bretschneideer spectrum, ITTC(International Towing Tank Conference) single parameter spectrum, ITTC dual parameter spectrum, and JONSWAP spectrum. PM spectrum is used to describe the waves generated by fully grown wind [37], which is widely used in ship engineering, the expression is

$$S(\rho) = A\rho^{-5}\exp(-B\rho^{-4}) \tag{38}$$

$$S(\rho_e) = \frac{S(\rho)}{\left|1 + \frac{2\rho}{g}U\cos\varsigma\right|} \tag{39}$$

ρ is the wave normalized frenquency, $A = 8.1 \times 10^{-3}g^2, B = 0.74(g/V_{19.4})^4 = 3.11/H_s^2$, H_s is wave height, $V_{19.4}$ is the wind speed at 19.4m above sea level, U is ship velocity, ς is the encounter angle between ship heading and wave. In the simulation part, $\xi = 8.75$, $H_s = 3m$, $U = 7.2m/s$.

The formula for calculating the peak wave frequency is as follows:

$$\rho_p = \sqrt[4]{\frac{4B}{5}} \tag{40}$$

According to equations (39) and (40), the peak frequencies corresponding to different wave heights are calculated as shown in Table 1.

The corresponding wave spectrum at different wave heights can be got according to formula (39) and Table 1.

The simulation results are shown as follows:

As shown in Figure 5 and Figure 6, when there is external interference, the tracking curve only has a small deviation from the expected curve trajectory, and there is no oscillation, the curve is smooth, and the control accuracy is high. The controller can gradually track the desired trajectory under

TABLE 1. Wave hight vs. peak frequency.

$V_{19.4}/(m\cdot s^{-1})$	11.8	13.7	15.3	16.7	18.1
H_s/m	3.0	4.0	5.0	6.0	7.0
$\rho_p/(rad\cdot s^{-1})$	0.725	0.628	0.562	0.513	0.475

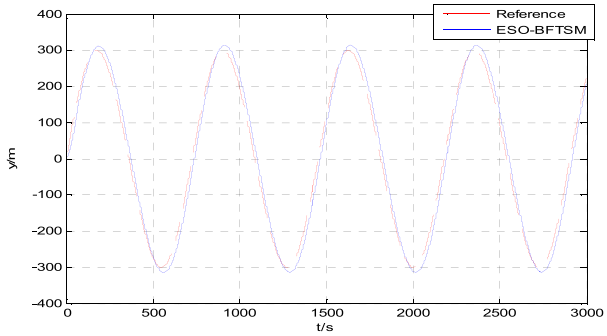

FIGURE 5. Lateral position comparison.

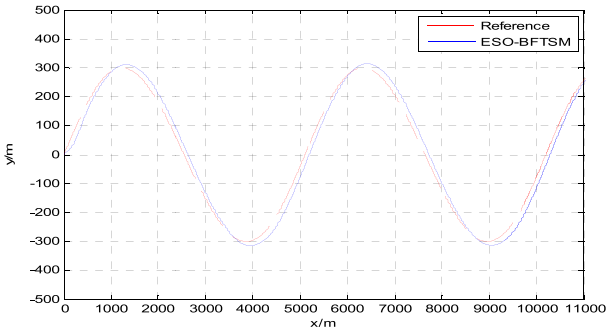

FIGURE 6. Ship position trajectory.

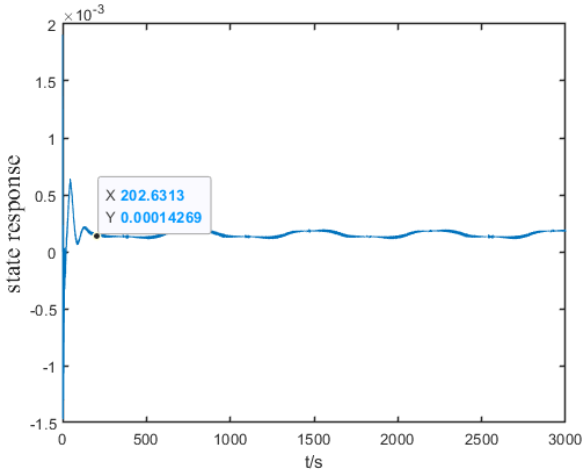

FIGURE 7. Convergence time of the sliding surface.

external disturbance, which meets the expected maritime practice requirements.

As shown in Figure 7, the convergence time of the sliding surface is 202s, and the system can achieve stable state quickly.

Fig. 8 and Fig. 9 show the change of the rudder angle and course of the ESO-FTSM control system, respectively.

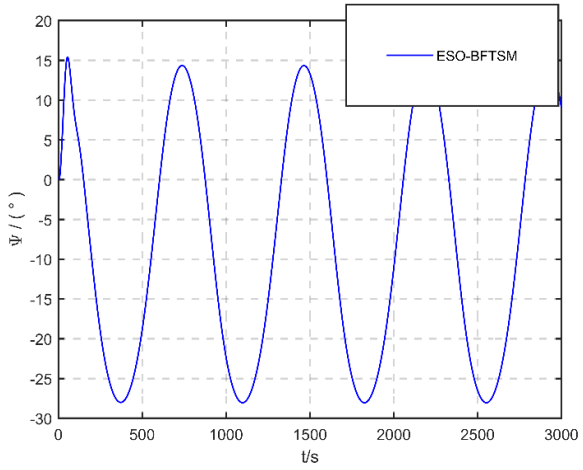

FIGURE 8. Heading angel.

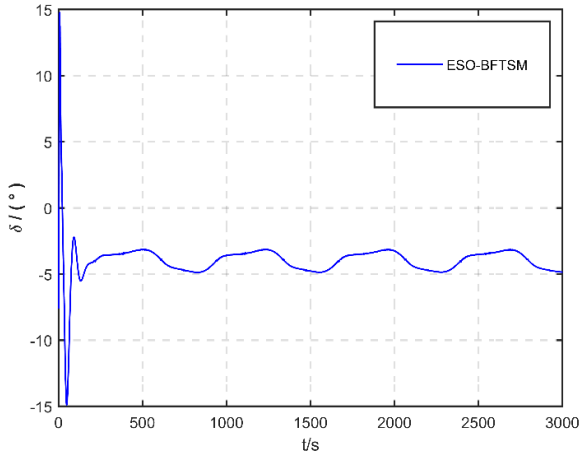

FIGURE 9. Rudder angel.

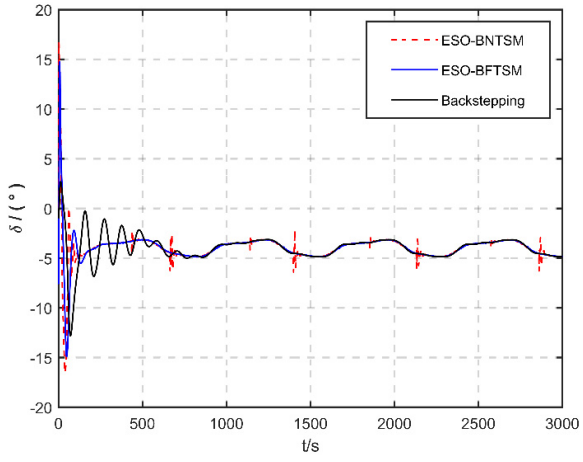

FIGURE 10. Rudder angle comparison.

From the above simulation results, it can be seen that: The rudder angle changes in a small range and the maximum change range is −14.8-15. A smooth periodic curve is formed at 150s to avoid frequent steering rudder angle wear and tear on the steering gear; the heading curve is soft and a regular curve is constructed at 200 s.

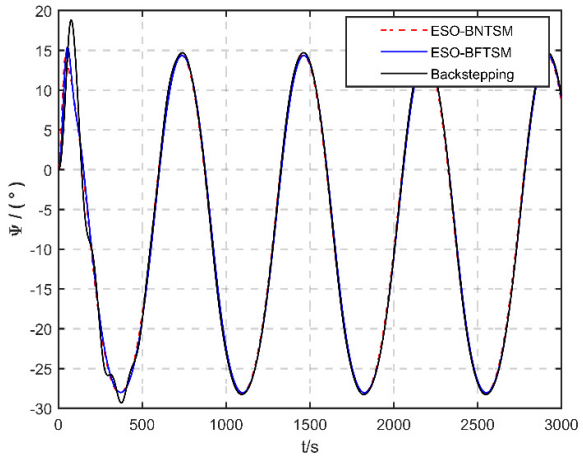

FIGURE 11. **Heading angle comparison.**

On the other side, to further verify the effectiveness of the ESO-FTSM control algorithm, simulation environment remains unchanged, the control effects of the ESO-NTSM based tracking controller, the ESO-FTSM based tracking controller and the bsckstepping based tracking controller are compared. The simulation rusults are shown as follows.

It can be seen from Figure 10-11 that both the ESO-BFTSM controller and the ESO-BNTSM controller can quickly and accurately track the curve track under the external disturbances, and the heading curve is stable and smooth. The heading angle caused by the ESO-BFTSM based controller is more smoothly. Moreover, the rudder angle of the ESO-BFTSM controller is softer than the ESO-BNTSM controller, with less oscillation and no chattering in the steady state. It shows that the selected FTSM and the new continuous control law can improve the dynamic quality effectively, and avoide the system chattering at the equilibrium point, and it's more robust.

V. CONCLUSION

A DSC-ESO approach based on the sliding mode control for the surface ship was proposed in this paper. And it constructed the expected yaw heading equation, established the mathematical relationship between the desired heading and the track deviation, and achieved the purpose of ship tracking control ultimately. The ESO could observe and estimate the disturbances of the system in real-time. The adoption of FTSM during the Backstepping progress improved the convergence speed of the controller, and the designed continuous control law solved the chattering problem well. The simulation results proved that the ESO-BFTSM controller had strong robustness and could track complex curved track quickly and accurately with high control quality.

REFERENCES

[1] T. Li, R. Zhao, C. L. P. Chen, L. Fang, and C. Liu, "Finite-time formation control of under-actuated ships using nonlinear sliding mode control," *IEEE Trans. Cybern.*, vol. 48, no. 11, pp. 3243–3253, Nov. 2018.

[2] W. Bai, J. Ren, T. Li, and C. L. P. Chen, "Grid index subspace constructed locally weighted learning identification modeling for high dimensional ship maneuvering system," *ISA Trans.*, vol. 86, pp. 144–152, Mar. 2019.

[3] Y. Li, S. Tong, and T. Li, "Hybrid fuzzy adaptive output feedback control design for uncertain MIMO nonlinear systems with time-varying delays and input saturation," *IEEE Trans. Fuzzy Syst.*, vol. 24, no. 4, pp. 841–853, Aug. 2016.

[4] C. L. P. Chen and S. Feng, "Generative and discriminative fuzzy restricted Boltzmann machine learning for text and image classification," *IEEE Trans. Cybern.*, vol. 50, no. 5, pp. 2237–2248, May 2020.

[5] V. G. Rubio, J. A. R. Ferrán, J. M. M. García, N. S. Almodóvar, J. M. L. Mayordomo, and F. Álvarez, "Automatic change detection system over unmanned aerial vehicle video sequences based on convolutional neural networks," *Sensors*, vol. 19, no. 20, pp. 4484–4500, 2019.

[6] Y. Yang, "A time-specified nonsingular terminal sliding mode control approach for trajectory tracking of robotic airships," *Nonlinear Dyn.*, vol. 92, no. 3, pp. 1359–1367, May 2018.

[7] Z. Hou, P. Lu, and Z. Tu, "Nonsingular terminal sliding mode control for a quadrotor UAV with a total rotor failure," *Aerosp. Sci. Technol.*, vol. 98, Mar. 2020, Art. no. 105716.

[8] Y. Yang and Y. Yan, "Attitude regulation for unmanned quadrotors using adaptive fuzzy gain-scheduling sliding mode control," *Aerosp. Sci. Technol.*, vol. 54, pp. 208–217, Jul. 2016.

[9] A. Maki, Y. Akimoto, and U. Naoya, "Application of optimal control theory based on the evolution strategy (CMA-ES) to automatic berthing (part: 2)," *J. Mar. Sci. Technol.*, vol. 25, pp. 221–233, Oct. 2020.

[10] H. Lyu and Y. Yin, "COLREGS-constrained real-time path planning for autonomous ships using modified artificial potential fields," *J. Navigat.*, vol. 72, no. 3, pp. 588–608, May 2019.

[11] Y. Wen, Z. Sui, C. Zhou, C. Xiao, Q. Chen, D. Han, and Y. Zhang, "Automatic ship route design between two ports: A data-driven method," *Appl. Ocean Res.*, vol. 96, Mar. 2020, Art. no. 102049.

[12] G. Piao, C. Guo, and S. Sun, "Research into the automatic berthing of underactuated unmanned ships under wind loads based on experiment and numerical analysis," *J. Marine Sci. Eng.*, vol. 7, no. 9, pp. 300–322, 2019.

[13] X. Wu, H. Chen, C. Chen, M. Zhong, S. Xie, Y. Guo, and H. Fujita, "The autonomous navigation and obstacle avoidance for USVs with ANOA deep reinforcement learning method," *Knowl.-Based Syst.*, vol. 196, May 2020, Art. no. 105201.

[14] A. Haseltalab and R. R. Negenborn, "Adaptive control for autonomous ships with uncertain model and unknown propeller dynamics," *Control Eng. Pract.*, vol. 91, Oct. 2019, Art. no. 104116.

[15] H. Q. Nguyen, A. D. Tran, and T. T. Nguyen, "The bilinear model predictive method-based motion control system of an underactuated ship with an uncertain model in the disturbance," *Processes*, vol. 7, no. 7, pp. 445–459, 2019.

[16] Y. Teng, "Research on mathematical model and dynamic positioning control algorithm of six degrees of freedom maneuvering in marine ships," *J. Intell. Fuzzy Syst.*, vol. 38, no. 2, pp. 1299–1309, Feb. 2020.

[17] T. Soni, A. S. Das, and J. K. Dutt, "Active vibration control of ship mounted flexible rotor-shaft-bearing system during seakeeping," *J. Sound Vibrat.*, vol. 467, Feb. 2020, Art. no. 115046.

[18] Z. Chen, B. Qin, M. Sun, and Q. Sun, "Q-Learning-based parameters adaptive algorithm for active disturbance rejection control and its application to ship course control," *Neurocomputing*, vol. 408, pp. 51–63, Sep. 2020.

[19] M. Zhu, A. Hahn, and Y.-Q. Wen, "Identification-based controller design using cloud model for course-keeping of ships in waves," *Eng. Appl. Artif. Intell.*, vol. 75, pp. 22–35, Oct. 2018.

[20] Z. Liu, "Ship course keeping using different sliding mode controllers," *Trans. FAMENA*, vol. 43, no. 2, pp. 49–60, Jul. 2019.

[21] Z. Zhao and Q. Zhang, "Adaptive self-regulation PID tracking control for the ship course," *Chin. J. Ship Res.*, vol. 14, no. 3, pp. 145–151, 2019.

[22] Y. Ma, G. Zhu, and Z. Li, "Error-driven-based nonlinear feedback recursive design for adaptive NN trajectory tracking control of surface ships with input saturation," *IEEE Intell. Transp. Syst. Mag.*, vol. 11, no. 2, pp. 17–28, Summer 2019.

[23] N. Wang and Z. Deng, "Finite-time fault estimator based fault-tolerance control for a surface vehicle with input saturations," *IEEE Trans. Ind. Informat.*, vol. 16, no. 2, pp. 1172–1181, Feb. 2020.

[24] X. Sun, G. Wang, and Y. Fan, "Model identification and trajectory tracking control for vector propulsion unmanned surface vehicles," *Electronics*, vol. 9, no. 1, pp. 22–35, 2019.

[25] L. Chen, R. Cui, C. Yang, and W. Yan, "Adaptive neural network control of underactuated surface vessels with guaranteed transient performance: Theory and experimental results," *IEEE Trans. Ind. Electron.*, vol. 67, no. 5, pp. 4024–4035, May 2020.

[26] M. Li, T. Li, X. Gao, Q. Shan, C. L. P. Chen, and Y. Xiao, "Adaptive NN event-triggered control for path following of underactuated vessels with finite-time convergence," *Neurocomputing*, vol. 379, pp. 203–213, Feb. 2020.
[27] C. Liu, C. L. P. Chen, Z. Zou, and T. Li, "Adaptive NN-DSC control design for path following of underactuated surface vessels with input saturation," *Neurocomputing*, vol. 267, pp. 466–474, Dec. 2017.
[28] Z. Shen, Y. Bi, Y. Wang, and C. Guo, "MLP neural network-based recursive sliding mode dynamic surface control for trajectory tracking of fully actuated surface vessel subject to unknown dynamics and input saturation," *Neurocomputing*, vol. 377, pp. 103–112, Feb. 2020.
[29] J.-W. Li, "Robust adaptive control of underactuated ships with input saturation," *Int. J. Control*, pp. 1–10, Oct. 2019.
[30] S. Xie, X. Chu, C. Liu, J. Liu, and J. Mou, "Parameter identification of ship motion model based on multi-innovation methods," *J. Mar. Sci. Technol.*, vol. 25, no. 1, pp. 162–184, Mar. 2020.
[31] X.-K. Zhang and Y.-C. Jin, "Transfigured loop shaping controller and its application to underwater vehicle," *Int. J. Autom. Comput.*, vol. 2, no. 1, pp. 48–51, Jul. 2005.
[32] J. Ning, J. Sun, T. Li, and W. Qiao, "Ship's track keeping based on variable structure active-disturbance rejection control," in *Proc. 6th Int. Conf. Intell. Control Inf. Process. (ICICIP)*, Nov. 2015, pp. 421–425.
[33] R. Li, J. Cao, and T. Li, "Active disturbance rejection control design and parameters configuration for ship steering with wave disturbance," *Control Theory Appl.*, vol. 35, no. 11, pp. 1601–1609, 2018.
[34] B. Qiu, G. Wang, Y. Fan, D. Mu, and X. Sun, "Path following of underactuated unmanned surface vehicle based on trajectory linearization control with input saturation and external disturbances," *Int. J. Control Automat. Syst.*, vol. 18, pp. 2108–2119, Feb. 2020.
[35] T. Li, Z. Li, D. Wang, and C. L. Philip Chen, "Output-feedback adaptive neural control for stochastic nonlinear time-varying delay systems with unknown control directions," *IEEE Trans. Neural Netw. Learn. Syst.*, vol. 26, no. 6, pp. 1188–1201, Jun. 2015.
[36] L. Qiao and W. Zhang, "Trajectory tracking control of AUVs via adaptive fast nonsingular integral terminal sliding mode control," *IEEE Trans. Ind. Informat.*, vol. 16, no. 2, pp. 1248–1258, Feb. 2020.
[37] J. Prendergast, M. Li, and W. Sheng, "A study on the effects of wave spectra on wave energy conversions," *IEEE J. Ocean. Eng.*, vol. 45, no. 1, pp. 271–283, Jan. 2020.

JUN NING received the B.S. degree in navigation technology and the master's degree in traffic information engineering and control from Dalian Maritime University (DMU), Dalian, China, in 2011 and 2013, respectively, and the master's degree in maritime safety and environment administration from World Maritime University (WMU), Malmo, Sweden, in 2018. He is currently pursuing the doctor's degree in traffic engineering with DMU.

He has been a Lecturer with DMU, since 2013. Moreover, he is also a seman and holds the third officer's certificate for ocean going vessel. His research interests include ship intelligent control, multi-agent systems, and automatic ship collision avoidance.

HANMIN CHEN was born in Zhejiang, China, in 1997. He received the B.S. degree in navigation technology from Zhejiang Ocean University, Zhoushan, China, in 2019. He is currently pursuing the M.S. degree in traffic information engineering and control with Dalian Maritime University, Dalian, China. His research interests include the ship intelligent collision avoidance and automatic control systems.

WEI LI received the B.S. degree in navigation technology, the master's degree in traffic information engineering and control, and the Ph.D. degree in traffic engineering from Dalian Maritime University (DMU), Dalian, China, in 1991, 2001, and 2014, respectively.

He was a Lecturer with DMU, from September 1991 to June 2004, and an Associate Professor from 2004 to 2013. As a one year visiting Scholar, he visited Tokyo Mercantile Marine University, Tokyo, Japan, in 2003. Since July 2013, he has been a Full Professor with DMU. He has also been a Lecturer with DMU, since 2013. Moreover, he is also a seman and holds the third officer's certificate for ocean going vessel. His research interests include ship intelligent control, multi-agent systems, and automatic ship collision avoidance. Moreover, he is also a seman and holds the chief officer's certificate for ocean going vessel. His research interests also include ship intelligent control, automatic ship collision avoidance, and ship's manoeuverability.

BAISONG DU received the master's degree in navigation science and technology from Dalian Maritime University, Dalian, China, in 2017.

He is currently a Lecturer with the School of Port and Transportation Engineering, Zhejiang Ocean University, Zhoushan, China. He is also an ocean-going ship captain with 11 years' sea service. His research interests include applied predictive modeling, ship intelligent control, and automatic ship collision avoidance.